Advances in Concrete Construction, *Vol. 12, No. 1* (*2021*) *63-74*
https://doi.org/10.12989/acc.2021.12.1.063

Shear strengthening of reinforced concrete beams using NSM/EBR techniques

Ahmed H. Abdel-kareem[a], Ahmed S. Debaiky[b], Mohamed H. Makhlouf[c] and M. Abdel-baset[*]

Department of Civil Engineering, Benha Faculty of Engineering, Benha University, Egypt

(*Received April 1, 2019, Revised February 10, 2021, Accepted May 31, 2021*)

Abstract. This paper presents the experimental results of research into the behavior of shear-enhanced reinforced concrete R.C beams using steel stirrups, Fiber Reinforced Polymers FRP rods, and Fiber Reinforced Polymers FRP strips. This enhancement was accomplished by the Near Surface Mounted technique NSM. The NSM technique contains a groove on the outside surface of the concrete member to adjust the depth to be less than the cover of the member. After cleaning, the epoxy paste was used to fill half of the groove's depth. In the groove, the particular FRP element is then installed. Finally, the groove is filled with epoxy and the outside surface of the concrete is levelled with so much epoxy. This method enables the fiber reinforcement polymer FRP materials is covered completely by epoxy. The objective of this research is to study the effect of NSM technique on shear resistance for stressed beam. 13 experimental studies of half-scale R.C beams were involved in this paper. The experimental program included two specimens strengthened with steel stirrups, eight specimens strengthened with stirrups of Glass Fiber Reinforced Polymer GFRP rods with the shape of deferent end anchorage and angle, two specimens strengthened with externally bonded GFRP strips. The remaining un-strengthened specimen was allocated for comparison as a control one. The test results included ultimate load of capacity, deflection, cracking, and failure mode. All beams enhanced with GFRP rods showed a capacity improvement ranging from 14% to 85% compared to the reference beam, and compared to the reference beam, beams enhanced with GFRP strips showed a capacity improvement ranging from 7% to 22%.

Keywords: fiber reinforced polymer FRP; near surface mounted NSM; reinforced concrete RC; shear; strengthening

1. Introduction

Due to harsh environmental conditions, many existing reinforced concrete elements are exposed to damage. These involve high temperatures, humidity, and salt-water penetration. Such harsh environmental conditions contribute to serious degradation of concrete buildings, mostly due to problems with steel corrosion, Al-Salloum *et al.* (2013). Shear failure is catastrophic and normally happens without warning in advance. It is also desirable that the beam fails in flexure rather than in shear. Shear deficiencies occur for many reasons, including inadequate shear reinforcement or reduction due to corrosion, increased service load, and building defects. It is expensive to Repairing these elements and a many of strengthening procedures have been carried out to repair the degraded elements formerly. such as increasing the cross-section of stirrups and installing additional steel plates, which is a waste of time and cost. Because of the ease of installation and economic viability of these methods, external stirrups and additional externally bonded steel plates using epoxy were used at the beginning to improve the load carrying capacity of reinforced concrete members. However, Due to probable corrosion, heavy-weight and practical difficulties with regard to external post-tensioning, these techniques showed reliability limitations.

Therefore, the need for a material free of corrosion for retrofitting techniques emerged. In aerospace applications, developments in fiber-reinforced polymer FRP composites have drawn attention to their potential in civil engineering applications. FRP resistant to corrosion and thus help us to improve strength and durability. Generally, the FRP materials consist of fibers that are impregnated in the matrix of vinyl ester which convert the loads between the fibers and protect them. The fibers could be made from glass, aramid, and Carbone.

Using an externally bonded reinforcement EBR technique, sheets, and laminates of FRP are usually applied on the faces of the elements to be enhanced in order to increase the shear resistance of concrete beams. Several researchers have confirmed that by following the EBR technique the shear resistance of concrete beams can be greatly improved. Over the past two decades, shear and/or flexural strengthening with externally bonded FRP laminates have become a celebrated and promising technique owing to extensive experimental tests Mosallam and Banerjee (2007), Eslami and Ronagh (2014), Mostofinejad and mahmoudabadi (2010), Moshiri, N *et al* (2019), analytical investigations Dalalbashi *et al*. (2012),

*Corresponding author, MSc Graduate
E-mail: mo.baset@yahoo.com
[a]Professor
E-mail: ahassan_k64@yahoo.com
[b]Professor
E-mail: debaiky@hotmail.com
[c]Assistant Professor
E-mail: mohamedmakhlouf83@yahoo.com

ISSN: 2287-5301 (Print), 2287-531X (Online)

Deng *et al*. (2016), Kocak (2015), and nonlinear finite element models Baji *et al*. (2015), Dalalbashi *et al*. (2013) conducted in the field. But this technique cannot mobilize the full tensile strength of FRP materials, due to premature debonding from the concrete substrate. Since FRP systems are directly exposed to weathering conditions, negative influences of freeze/thaw cycles and the effect of high and low temperatures should be considered in the reinforcing performance of these materials. In addition, EBR systems are susceptible to fire and act of vandalism.

Near surface mounted NSM technique had been also introduced as a more efficient alternative in FRP strengthening of RC beams Dias and Barros (2013), Bianco *et al*. (2014), Ramezanpour *et al*. (2018), Al Rjoub *et al*. (2019). In this technique, a pre-cut groove using saw is made on the tension surface/face of the beam. The groove is half filled with construction adhesive, and then FRP bar is pressed inside the grove such that half of the circumferential perimeter of the bar is covered with adhesive. Thereafter, the groove is then completely filled with adhesive. NSM had been suggested as a promising technique for improving the performance of structurally deficient R.C structure, because of its ease of installation. However, research showed that the performance of this technique is strongly dependent on the bond performance between epoxy-concrete and epoxy-FRP rod. The literature includes numerous studies on the efficiency of FRP as shear reinforcement. The reinforcement technique using CFRP sheets can be used to increase the shear capacity significantly, as per Khalifa and Nanni (2002). Rizzo and De Lorenzis (2009) suggested that the NSM FRP reinforcement significantly enhanced the shear capacity of RC beams also in the presence of a limited amount of steel shear reinforcement. De Lorenzis and Teng (2007) have discussed the issues raised by the use of NSM FRP reinforcement such as optimization of construction details, models for the bond behavior between NSM FRP and concrete, reliable design models for flexural and shear strengthening and the maximization of the advantages of this technique. They also gave a critical review of existing research in this area, identified gaps of knowledge, and outlined directions for further research. The study by Jayaprakash *et al*. (2008) confirmed that the bi-directional CFRP strip strengthening technique contributes shear capacity to reinforced concrete rectangular shear beams. The study also showed that the external CFRP strip acts as shear reinforcement similar to the internal steel stirrups. Hassan and Rizkalla (2002) investigated the feasibility of using different strengthening techniques as well as different types of FRP for strengthening concrete structures. Test results showed that the efficiency of NSM CFRP strips was three times that of the EBR CFRP strips. Kachlakev and McCurry (2000) showed that the addition of GFRP alone for shear was sufficient to offset the lack of steel stirrups and allow conventional RC beam failure by yielding of the tension steel. Sundarraja and Rajamohan (2009) have conducted experiments on reinforced concrete beams externally strengthened with GFRP inclined strips as shear reinforcements. The effectiveness of side strips was compared with that of the U-wrap strips. The ultimate loads of beams retrofitted with Uwrapping were greater than the beams retrofitted by bonding the GFRP strips on the sides alone. The test results by Täljsten and Elfgren (2000) proved that a very good strengthening effect in shear could be achieved by bonding fabrics to the face of concrete beams. Hassan and Rizkalla (2003) showed that the use of NSM CFRP strips substantially increases the stiffness, strength, debonding loads and bond characteristics of concrete beams. Zhang and Hsu (2005) concluded that the FRP system can significantly increase the serviceability, ductility, and ultimate shear strength of a concrete beam. Thus, restoring beam shear strength by using FRP is an effective technique.

2. Experimental program

The implementation of the Near Surface Mounted reinforcement technique to improve the shear resistance of concrete beams using GFRP is subject of the research. The NSM technique is based on the fixation of GFRP in cut slits opened with adhesive on the concrete cover of the lateral surfaces of the beams. An experimental program on reinforced concrete beams that failed to shear was carried out to test the effectiveness of this technique. One beam was taken as a non-reinforced reference beam. The beams strengthened by the NSM method have been divided into two parts of beam specimens. The first series, series A consists of ten strengthened beam specimens. two specimens strengthened with steel stirrups at spacing 200 mm and 150 mm respectively, two specimens each were strengthened with NSM GFRP rods with U-shape at angle 90° and 45° respectively, two specimens each were strengthened with NSM GFRP rods with U-shape with cap at angle 90° and 45° respectively, two specimens each were strengthened with NSM GFRP rods with U-shape with anchorage at angle 90° and 45° respectively, two specimens each were strengthened with NSM GFRP rods with U-shape with strand at angle 90° and 45° respectively. The second series, series B consists of two strengthened beam specimens. two specimens each were strengthened with EBR GFRP strips with Box-shape and U-shape with the top rod at angle 90°respectively. As shown in Table 1.

2.1 Details of specimens

The beam size that was chosen for the experiment was 150 mm×300 mm×1700 mm, the beams were designed to be shear-deficient beams. Three numbers of 16 mm diameter bars were put as tension reinforcement, and two numbers of 10 mm diameter bars were put as top reinforcement. Three-legged 6 mm diameter bars were put as holding stirrups at both ends of the beam and middle. as shown in Fig. 1.

2.2 Materials

The specimens used in the test program were cast using normal strength concrete with cube strength of 40 MPa. The strengthening materials used were high grade steel, GFRP

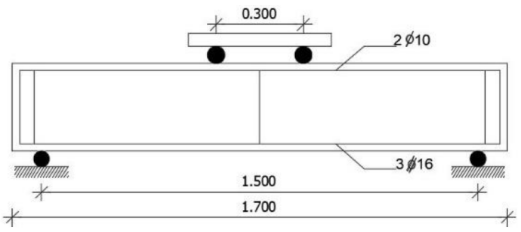

B-CO

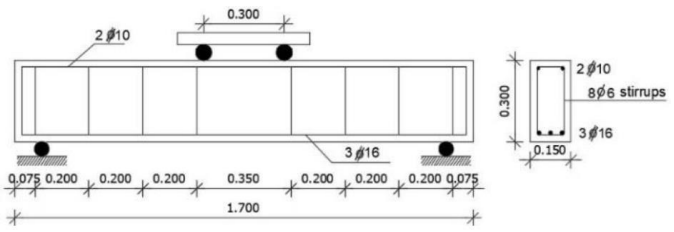

S8-90

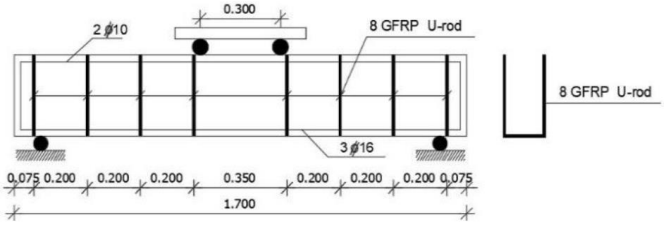

GR8-U-90

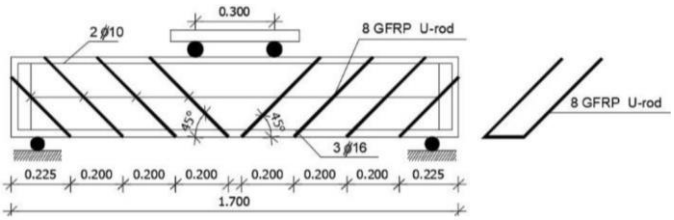

GR8-U-45

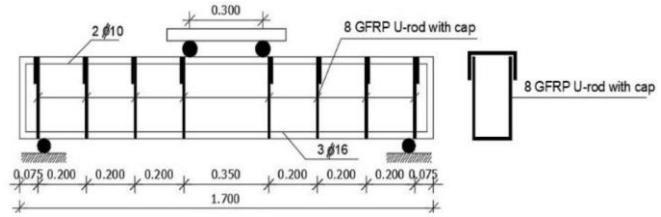

GR8-UC-90

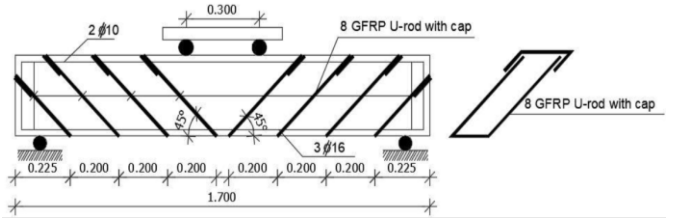

GR8-UC-45

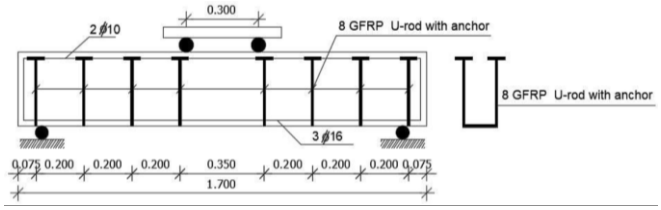

GR8-UA-90

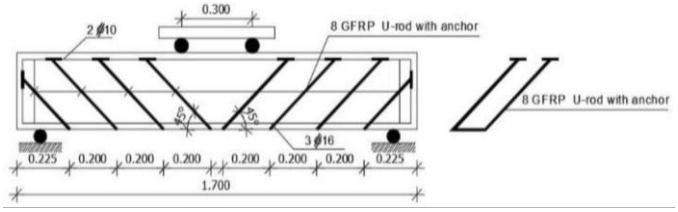

GR8-UA-45

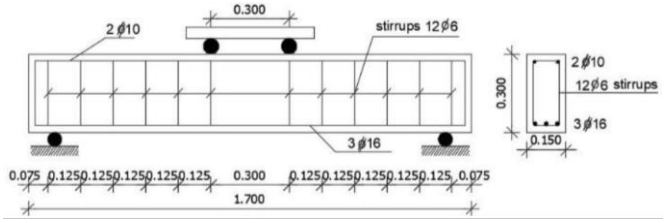

S12-90

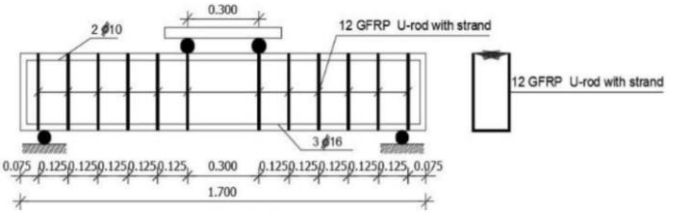

GR12-UD-90

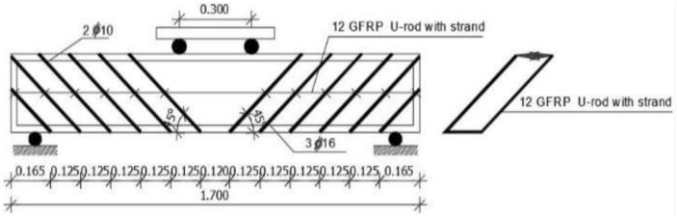

GR12-UD-45

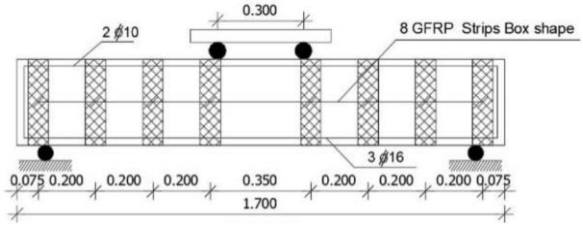

GS8-B-90

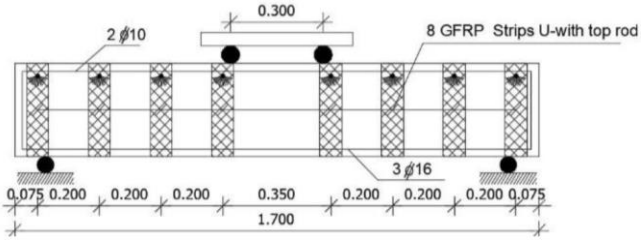

GS8-UR-90

Fig. 1 Dimensions and details of reinforcement of specimens

Table 1 The distribution of the reinforced concrete beams of the test program

Group	Specimen code	Specimen Case	Material	Shape	Spacing (mm)	Angle
Control	B-CO	Control	------	------	---	---
A	S8-90	Strengthening beams with NSM	Steel	8Ø6 two branches	200	90
	GR8-UC-90		GFRP	8 Rod (U - shape with cap)	200	90
	GR8-UC-45		GFRP	8 Rod (U - shape with cap)	200	45
	GR8-U-90		GFRP	8 Rod (U - shape)	200	90
	GR8-U-45		GFRP	8 Rod (U - shape)	200	45
	GR8-UA-90		GFRP	8 Rod (U- shape with anchorage)	200	90
	GR8-UA-45		GFRP	8 Rod (U– shape with anchorage)	200	45
	S12-90		Steel	12Ø6 two branches	125	90
	GR12-UD-90		GFRP	12 Rod (U- shape with strand)	125	90
	GR12-UD-45		GFRP	12 Rod (U– shape with strand)	125	45
B	GS8-B-90	EBR	GFRP	8 Strips (Box- shape)	200	90
	GS8-UR-90		GFRP	8 Strips (U- shape with top rod)	200	90

Table 2 Characteristic properties of steel bars, GFRP rods and GFRP sheets

(a) Characteristic properties of steel bars:

Nominal diameter (mm)	Actual area (mm^2)	Yield strength (N/mm^2)	Ultimate strength (N/mm^2)
Φ6	28.3	540	694
Φ10	78.5	490	795
Φ16	201	378	696

(b) Characteristic properties of GFRP rods

characteristic		GFRP rods
Diameter of bars	(mm)	6
Area of fibers	(mm^2)	6.06
Tensile strength	(N/mm^2)	1375
Modulus elasticity	(N/mm^2)	66245

(c) Characteristic properties of GFRP sheets

characteristic		GFRP Sheets
Fabric width	(mm)	600
Fabric thickness	(mm)	0.17
Tensile strength	(N/mm^2)	2300
Modulus elasticity	(N/mm^2)	76000

rods and strips. The mechanical properties of these materials were determined from tests carried out according to the specifications of the manufacturers, (Ezz Steel), (Sika Egypt), as shown in Table 2.

2.2.1 MMGFRP rods

2.2.1.1 Manufacturing of GFRP rods

The manually made GFRP rod MMGFRP was manufactured using FRP strips, where the glass fiber sheet was cut and then wrapped to form a 6 mm diameter rod. Initially, the required width of the FRP sheet (250 mm in this study) was calculated based on the design cross sectional area., The length of the FRP strip was equal to the length of the MMGFRP rod. A strip with the design width and length was cut from an FRP sheet, then wrapped and placed in the Wooden model on which the U-shaped grooved was to be manufactured. The mixed of two component epoxy resin was then put on the MMGFRP. After that, the trapped air was expelled. After it is finished, it is left to dry and then remove it from the Wooden model and manufacture other.

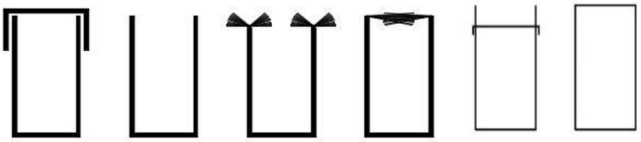

Fig. 2 different shapes of the end anchorage

Fig. 3 the end anchorage

2.2.1.2 MMGFRP anchorage

When the distance between NSM reinforcements in shear enhancement is large, the failure mode is usually NSM debonding, Dias and Barros (2010). In order to delay the debonding of MMGFRP rods when they are coarsely spaced, an innovative different end anchorage for the MMGFRP rods was proposed in this study. Fig. 2 shown the different shapes of the end anchorage. First, the MMGFRP rod is fabricated with glass fiber sheets and leave part of strip fiber at the end sides dry. Next, The MMGFRP is placed in the grooves on both sides of the beam, the dry fibers at the ends are impregnated with epoxy resin and placed in the grooves. The grooves at end anchorage are perpendicular to the MMGFRP rod when the MMGFRP rods are vertically installed. If the MMGFRP rods are installed not perpendicular to the beam axis, end anchorage is still manufactured to be parallel to the beam axis so in this case, the grooves at end anchorage are not perpendicular to the MMGFRP rod, as shown in Fig. 3. The main advantage of the proposed anchor system is that it only requires access to the surface of the beams for installation, so that it can be properly applied to RC beams whose top face is inaccessible, such as T-beams. With this anchoring, MMGFRP debonding may be delayed or prevented and more concrete is mobilized to contribute to

Fig. 4 cutting groove and placing MMGFRP rods

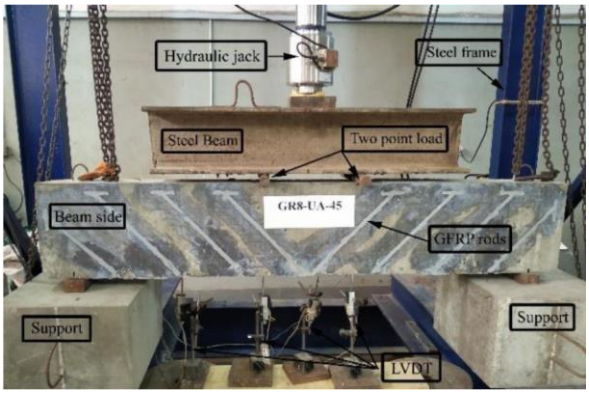

Fig. 5 Beam under test showing LVDT and hydraulic jack

the shear capacity of the beam.

2.3 Strengthening of specimens

In order to strengthen the shear deficient beams using the NSM technique and EBR technique for comparison, GFRP rods and GFRP strips were provided at various alignments. The Glass Fiber rods had tensile strength 2500 N/mm^2. The GFRP rod with different shape was provided at an angle 90° and 45° with the beam axis at the lateral faces for the shear strengthening of the beams. In order to apply the NSM technique, the precast grooves on the lateral surface of the beams were made rough, all grooves had a square cross section with a nominal depth and width of 10x10 mm. and then cleaned properly using a wire brush. Then the grooves were filled halfway with the groove filler. The surface of the GFRP rods was roughened for ensuring a proper bond between GFRP and the groove filler. Then GFRP is inserted into the groove, so the groove filler flows around the GFRP. Then the surface is leveled and smoothened. Then the strengthened beams were left to cure in air for seven days before testing. As shown in Fig. 4.

In order to strengthen the shear deficient beams using the EBR technique, U wrap of GFRP strips of size 750 mm×25 mm×0.17 mm were provided over the entire shear zones. The GFRP used for the EBR application of tensile strength 2300 N/mm^2.

2.4 Testing of specimens

For the test set-up used in this study consisted of rigid steel frames supported by the laboratory rigid floor. The

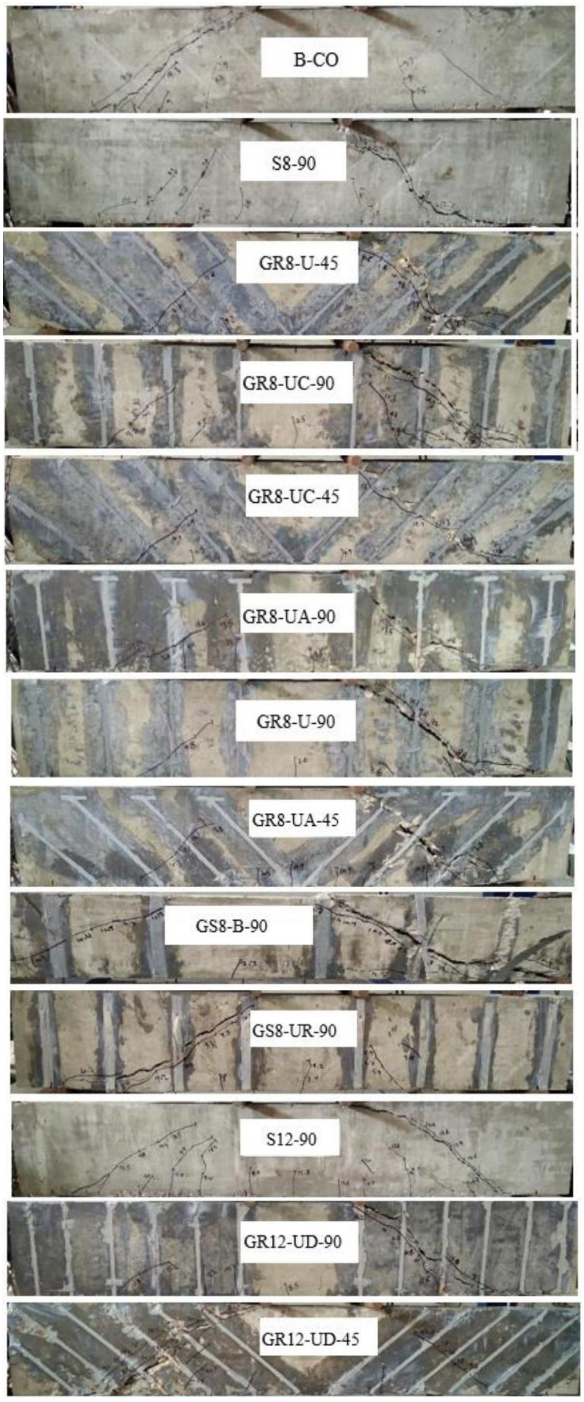

Fig. 6 Crack pattern in test of all beams

load was applied using a hydraulic jack of 1000 kN capacity, Load was measured using a load cell connected to the data acquisition system. The beam specimens were tested under two-point loading, as shown in Fig. 5. four linear variable differential transducers LVDT mounted at the bottom soffit of the specimen for measuring deflections, placed at mid-span of the specimen and under two load application points and mid-span of shear. Propagation of cracks was marked gradually up to failure.

3. Results and discussion

Table 3 Experimental results of specimens

Specimen code	P_{cr} (kN)	Δ_{cr} (mm)	P_{ul} (kN)	Δ_{ul} (mm)	Increase over reference beam without any shear reinforcement %				Increase over reference beam with steel stirrups %	
					$(P_{ul}/P_{ul\text{-}c})\%$	$(\Delta_{ul}/\Delta_{ul\text{-}c})\%$	$(P_{cr}/P_{cr\text{-}c})\%$	$(\Delta_{cr}/\Delta_{cr\text{-}c})\%$	$(P_{ul}/P_{ul\text{-}s})\%$	$(\Delta_{ul}/\Delta_{ul\text{-}s})\%$
B-CO	75.00	2.33	95.90	3.59	1.00	1.00	1.00	1.00	0.60	0.52
S8-90	76.50	2.60	160.40	6.93	1.67	1.93	1.02	1.12	1.00	1.00
GR8-U-90	78.00	3.47	109.50	5.58	1.14	1.55	1.04	1.49	0.68	0.81
GR8-U-45	93.00	3.00	112.00	5.22	1.17	1.45	1.24	1.29	0.70	0.75
GR8-UC-90	80.00	3.93	117.30	5.13	1.22	1.43	1.07	1.69	0.73	0.74
GR8-UC-45	99.00	2.82	120.70	4.06	1.26	1.13	1.32	1.21	0.75	0.59
GR8-UA-90	106.00	6.87	150.30	9.49	1.57	2.64	1.41	2.95	0.94	1.37
GR8-UA-45	112.00	4.74	169.03	8.13	1.76	2.26	1.49	2.03	1.05	1.17
GS8-B-90	76.50	2.89	116.65	5.72	1.22	1.59	1.02	1.24	0.73	0.83
GS8-UR-90	76.00	2.67	102.40	4.26	1.07	1.19	1.01	1.15	0.64	0.61
S12-90	86.00	1.74	203.20	7.29	2.12	2.03	1.15	0.75	1.00	1.00
GR12-UD-90	81.00	3.28	152.90	6.98	1.59	1.94	1.08	1.41	0.75	0.96
GR12-UD-45	84.50	2.39	177.80	6.73	1.85	1.87	1.13	1.03	0.88	0.92

Note: P_{cr}: Cracking load; Δ_{cr}: Deflection correspond to P_{cr}; Pul: Ultimate load; Δ_{ul}: Deflection correspond to P_{ul}

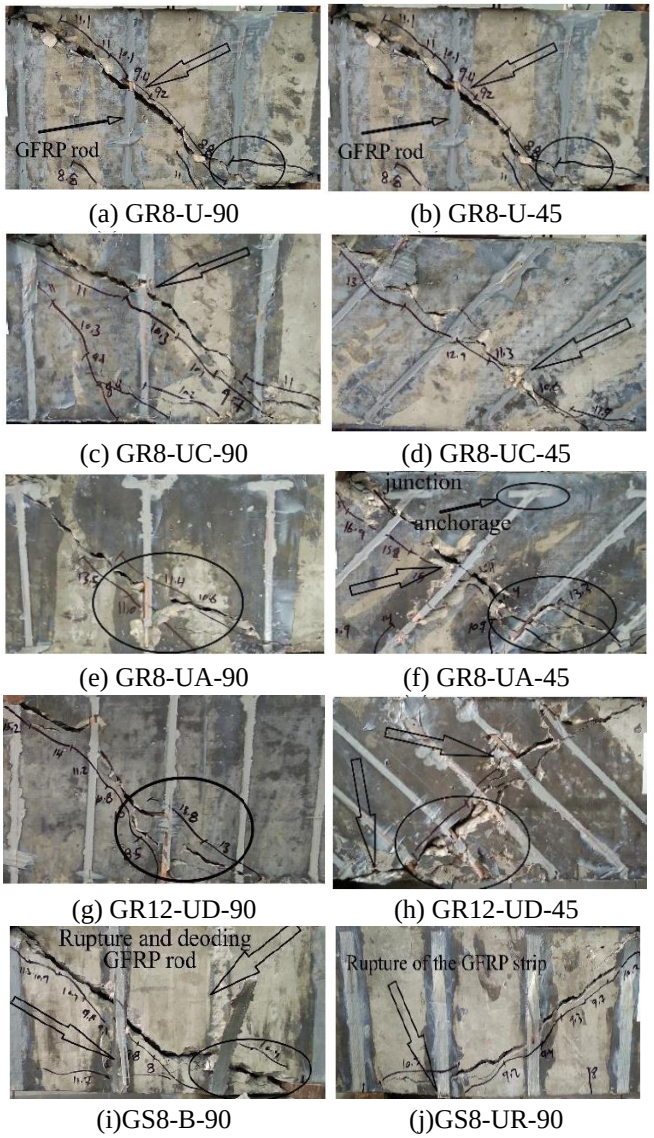

(a) GR8-U-90 (b) GR8-U-45

(c) GR8-UC-90 (d) GR8-UC-45

(e) GR8-UA-90 (f) GR8-UA-45

(g) GR12-UD-90 (h) GR12-UD-45

(i)GS8-B-90 (j)GS8-UR-90

Fig. 7 Close-up view of the failure modes

In this part, the observations during testing and the analysis of the results are briefly described.

3.1 Load–Carrying capacity of the tested specimens

The first crack load and ultimate load for the test specimens are shown in Table 3. Crack pattern in test of all beams showing in Fig. 6.

3.1.1 Control specimen B-CO

Flexural cracking in the reference beam started at the mid-span at a load of P=75 kN. The first shear crack appeared in about the middle of the test shear span at 82 kN. More flexural–shear cracks formed thereafter within the test shear span. At about 93 kN, these cracks had widened and propagated to form the final crack pattern. The beam failed in shear at P_{max}=95.9 kN. as shown in Table 3.

3.1.2 Series A

3.1.2.1 Specimen S8-90

For these beams strengthened with steel stirrups, the primary patterns of cracking were similar to that of the reference beam (B-CO), as shown in Fig. 6. the relationship between the maximum load and the deflection at beam mid-span is depicted in Fig. 8. Table 3 includes the main results obtained in this specimen. When compared to the maximum load of the (B-CO) beam, Table 3 show that the shear strengthening systems with steel stirrups increased the maximum load of 67% (S8-90). the crack load of this beam (S8-90) was 2% larger than the crack load of the (B-CO) beam. The deformation capacity was registered in the beam strengthened with steel stirrups corresponding to the max load. In comparison with Δ_{ul-c} (B-CO) beam, the Δ_{ul-s} is 93% larger. The deformation capacity corresponding to the crack load Δ_{cr-s} in this beam (S8-90) was 12% larger than the deformation capacity corresponding to the crack load in the (B-CO) beam Δ_{cr-c}.

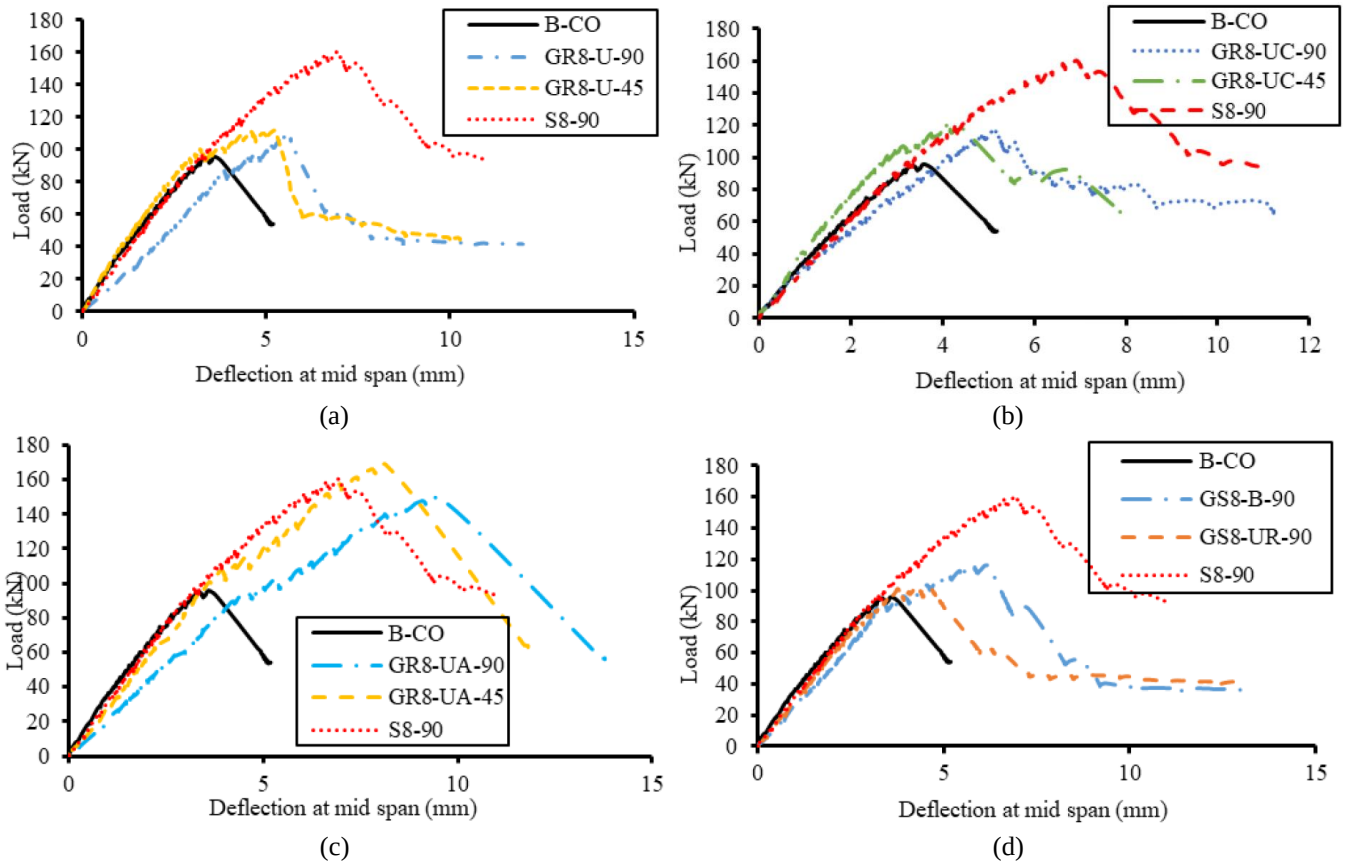

Fig. 8 Load-deflection relationship of series A

3.1.2.2 Specimens GR8-U-90 and GR8-U-45

For these beams strengthened with GFRP by NSM technique with rods (U–shape), Fig. 6 shown the crack pattern in these specimens. the relationship between the maximum load and the deflection at beam mid-span is depicted in Fig. 8(a). Table 3 includes the main results obtained in these specimens. Taking the maximum load of (B-CO) beam as a reference value, the (GR8-U-90), (GR8-U-45) beams provided a 14% and 17% increase in maximum load, respectively, as shown in Fig. 10. The crack load of these specimens (GR8-U-90), (GR8-U-45) was 4% and 24% larger than the crack load of the (B-CO) beam, respectively. when compared the maximum load in these specimens with beam strengthening with steel stirrups (S8-90) was 32% and 30% less than the maximum load in beam (S8-90). The deformation capacity was registered in the (GR8-U-90), (GR8-U-45) beams, corresponding to the maximum load at beam mid-span. In comparison with Δ_{ul-c} (B-CO) beam, the Δ_{ul} was 55% and 45% larger, respectively, as showing in Fig. 15. In comparison with Δ_{ul-s} (S8-90) beam, the Δ_{ul} was 19 % and 25 % less than the deformation capacity corresponding to the maximum load in the (S8-90) beam, respectively. The deformation capacity corresponding to the crack load Δ_{cr} in these beams (GR8-U90), (GR8-U-45) was 49% and 29% larger than the deformation capacity corresponding to the crack load in the (B-CO) beam Δ_{cr-c}. Finally, the specimens (GR8-U-90), (GR8-U-45) failed in shear at maximum load 109.5, 112 kN, respectively.

3.1.2.3 Specimens GR8-UC-90 and GR8-UC-45

For these beams strengthened with GFRP by (NSM) technique with rods U–shape with cap, Fig. 6 shown the crack pattern in these specimens. The relationship between the maximum load and the deflection at beam mid-span is depicted in Fig. 8(b). Table 3 includes the main results obtained in these specimens. Taking the maximum load of (B-CO) beam as a reference value, the (GR8-UC-90), (GR8-UC-45) beams provided a 22% and 26% increase in maximum force, respectively, as shown in Fig. 10. the crack load of these specimens (GR8-UC-90), (GR8-UC-45) was 7% and 32% larger than the crack load of the (B-CO) beam, respectively. when compared the maximum load in these specimens with beam strengthening with steel stirrups (S8-90) was 27% and 25% less than the maximum load in beam (S8-90). The deformation capacity was registered in the (GR8-UC-90), (GR8-UC-45) beams, corresponding to the maximum load at beam mid-span. In comparison with Δ_{ul-c}(B-CO) beam, the Δ_{ul} was 43% and 13% larger, respectively, as shown in Fig. 15. In comparison with Δ_{ul-s} (S8-90) beam, the Δ_{ul} was 26% and 41% less than the deformation capacity corresponding to the maximum load in the (S8-90) beam, respectively. The deformation capacity corresponding to the crack load Δ_{cr} in these beams (GR8-UC-90), (GR8-UC-45) was 69% and 21% larger than the deformation capacity corresponding to the crack load in the (B-CO) beam Δ_{cr-c}. Finally, the specimens (GR8-UC-90), (GR8-UC-45) failed in shear at maximum load 117.3, 120.7 kN, respectively. Although the use of the cap with GFRP

rods in these specimens, there was no significant improvement in the loading capacity in comparison to specimen (GR8-U-90), (GR8-U-45). As shown in Table 3.

3.1.2.4 Specimens GR8-UA-90 and GR8-UA-45

For these beams strengthened with GFRP by (NSM) technique with rods (U–shape with anchorage), Fig. 6 shown the crack pattern in these specimens. The relationship between the maximum load and the deflection at beam mid-span is depicted in Fig. 8(c). Table 3 includes the main results obtained in these specimens. Taking the maximum load of (B-CO) beam as a reference value, the (GR8-UA-90), (GR8-UA-45) beams provided a 57% and 76% increase in the maximum load, respectively, as shown in Fig. 10. where the highest value was registered in the beam strengthened with inclined rods with anchorage (GR8-UA-45). the crack load of these specimens was 41% and 49% larger than the crack load of the (B-CO) beam, respectively. When compared the maximum load in these specimens with beam strengthening with steel stirrups (S8-90), the beam (GR8UA-90) was 6% less than the maximum load in beam (S8-90), while the beam (GR8-UA-45) was the only one that achieved an increase of 5%. The deformation capacity was registered in the (GR8-UA90), (GR8-UA-45) beams, corresponding to the maximum load at beam mid-span. In comparison with Δ_{ul-c} (B-CO) beam, the Δ_{ul} was 164% and 126% larger, respectively, as shown in Fig. 15. In comparison with Δ_{ul-s} (S8-90) beam, the Δ_{ul} was 37% and 17% larger than the deformation capacity corresponding to the maximum load in the (S8-90) beam, respectively. The deformation capacity corresponding to the crack load Δ_{cr} in these beams (GR8-U-90), (GR8-U-45) was 195% and 103% larger than the deformation capacity corresponding to the crack load in the (B-CO) beam Δ_{cr-c}. Finally, the specimens (GR8-UA-90), (GR8-UA-45) failed in shear at maximum load 150.3, 169.03 kN, respectively. Registered with the highest load capacity, especially specimen (GR8-UA-45). Clearly the use of GFRP rods with anchored in (GR8-UA-90), (GR8-UA-45) beams led to a strengthening in both the ultimate strength and the corresponding deflection as shown in Table 3.

3.1.2.5 Specimens GS8-B-90 and GS8-UR-90

For these beams strengthened with GFRP by (EBR) technique with strips (Box–shape) and strips (U–shape with top rod), Fig. 6 shown the crack pattern in these specimens. the relationship between the maximum load and the deflection at beam mid-span is depicted in Fig. 8(d). Table 3 includes the main results obtained in these specimens. Taking the maximum load of (B-CO) beam as a reference value, the (GS8-B-90), (GS8-UR-90) beams provided a 22% and 7% increase in maximum load, respectively, as shown in Fig. 10. The (GS8-UR-90) specimen recorded the least load capacity. the crack load of these specimens (GS8-B-90), (GS8-UR-90) was 2% and 1% larger than the crack load of the (B-CO) beam, respectively. when compared the maximum load in these specimens with beam strengthening with steel stirrups (S8-90) was 27% and 36% less than the maximum load in beam (S8-90). The deformation capacity was registered in the (GS8-B-90), (GS8-UR-90) beams, corresponding to the maximum load at beam mid-span. In comparison with Δ_{ul-c} (B-CO) beam, the Δ_{ul} was 59 % and 19% larger, respectively, as shown in Fig. 15. In comparison with Δ_{ul-s} (S8-90) beam, the Δ_{ul} was 17% and 39% less than the deformation capacity corresponding to the maximum load in the (S8-90) beam, respectively. The deformation capacity corresponding to the crack load Δ_{cr} in these beams (GS8-B90), (GS8-UR-90) was 24% and 15% larger than the deformation capacity corresponding to the crack load in the (B-CO) beam Δ_{cr-c}. Finally, the specimens (GS8-B-90), (GS8-UR-90) failed in shear at the maximum load 116.65, 102.4 kN, respectively. by comparing the previous samples with samples (GS8-B-90) and (GS8-UA-90) it was observed that the NSM technique has an effective effect in shear resistance of the EBR technique.

3.1.3 Series B

3.1.3.1 Specimen S12-90

For this beam strengthened with steel stirrups Fig. 6 shown the crack pattern in this specimen, the relationship between the maximum load and the deflection at beam mid-span is depicted in Fig. 9. Table 3 includes the main results obtained in this. When compared to the maximum load of the (B-CO) beam, Table 3 shows that the shear strengthening systems with steel stirrups increased the maximum load of 112% (S12-90). the crack load of this beam (S12-90) was 15% larger than the crack load of the (B-CO) beam. The deformation capacity was registered in the beam strengthened with steel stirrups corresponding to the maximum load. In comparison with Δ_{ul-c} (B-CO) beam, the Δ_{ul-s} is 103 % larger. The deformation capacity corresponding to the crack load Δ_{cr-s} in this beam (S12-90) deformation capacity corresponding to the crack load in the (B-CO) beam Δ_{cr-c}.

3.1.3.2 Specimens GR12-UD-90 and GR12-UD-45

For these beams strengthened with GFRP by (NSM) technique with rods (U–shape with strand), Fig. 6 shown the crack pattern in these specimens, the relationship between the maximum load and the deflection at beam mid-span is depicted in Fig. 9. Table 3 includes the main results obtained in these specimens. Taking the maximum load of (B-CO) beam as a reference value, the (GR12-UD-90), (GR12-UD-45) beams provided a 59% and 85% increase in maximum load, respectively, as shown in Fig. 10. the crack load of these specimens (GR12-UD-90), (GR12-UD-45) was 8% and 13% larger than the crack load of the (B-CO) beam, respectively. when compared the maximum load in these specimens with beam strengthening with steel stirrups (S12-90) was 25% and 12% less than the maximum load in beam (S12-90). The deformation capacity was registered in the (GR12-UD-90), (GR12-UD-45) beams, corresponding to the maximum load at beam mid-span. In comparison with Δ_{ul-c} (B-CO) beam, the Δ_{ul} was 94% and 87% larger, respectively as shown in Fig. 15. In comparison with Δ_{ul-s} (S12-90) beam, the Δ_{ul} was 4% and 8% less than the deformation capacity corresponding to the maximum load in the (S12-90) beam, respectively. The deformation capacity corresponding to the crack load Δ_{cr} in these beams (GR12-UD-90), (GR12-UD-45) was 41% and 3% larger

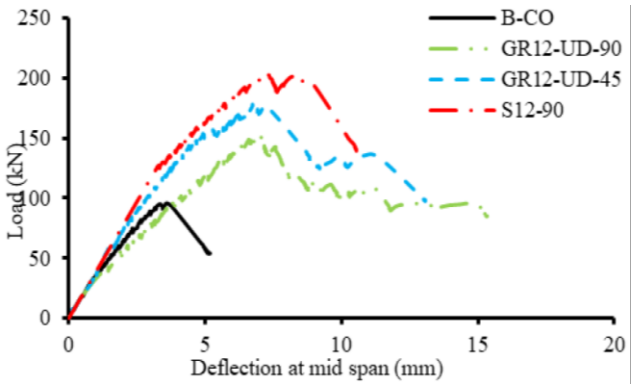

Fig. 9 Load-deflection at mid span relationship of series B

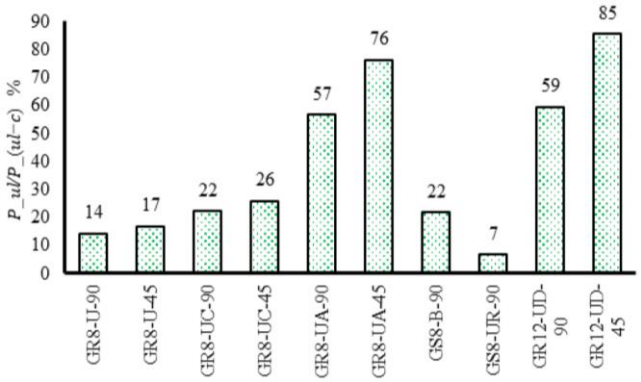

Fig. 10 influence of the strengthening using GFRP bars, strips

than the deformation capacity corresponding to the crack load in the (B-CO) beam Δ_{cr-c}. Finally, the specimens (GR12-UD-90), (GR12-UD-45) failed in shear at maximum load 152.9, 177.8 kN, respectively.

3.2 Failure modes

Figs. 6 and 7 shown the crack patterns and failure modes for all specimens. as was expected, all the tested specimens failed in shear, when the maximum load was reached, (B-CO) beam, without any reinforcement in shear, had failed by the formation of shear failure crack without the yielding of the longitudinal tensile reinforcement. A shear failure crack occurred in specimens strengthened with steel stirrups. However, in specimens (S8-90), (S12-90) this shear failure crack occurred after the yielding of the longitudinal tensile reinforcement. In specimens strengthened with GFRP rods with NSM technique, (GR8-U-90), (GR8-U-45) In these specimens the failure occurred due to the separation of large parts of concrete cover, but larger in (GR8-U-90). As shown in Figs. 7(a)-(b), respectively. In (GR8-UC-90), (GR8-UC-45) after the formation of the critical shear crack in these beams, debonding between GFRP rod and epoxy and separation for parts of concrete cover caused specimens to fail. As shown in Figs. 7(c)-(d), respectively. After the formation of the critical shear crack in beam (GR8-UA-90), the failure was not due to pure debonding between the GFRP rod and epoxy or the epoxy and concrete surface. Based on post-failure inspections, it was due to the formations of the crack in the concrete cover leading to the separation of part of concrete cover from the beam. as shown in Fig. 7(e). The beam (GR8-UA45) failed due to GFRP rod rupture at the junction between the GFRP rod and the anchorage as shown in Fig. 7(f). After this rupture occurred, some parts of the concrete cover surrounding the GFRP rod were peeled away. In (GR12-UD)-90, (GR12-UD-45). After the formation of the critical shear crack in these beams, the failure was due to debonding between the GFRP rod and epoxy. leading to the separation of a large part of concrete cover from the beam as shown in Figs. 7(g)-(h). After the formation of the critical shear crack in beam (GS8-B-90), the failure was due to debonding between the GFRP strip and concrete surface, rupture the GFRP. leading to the separation of a large part of concrete cover from the beam

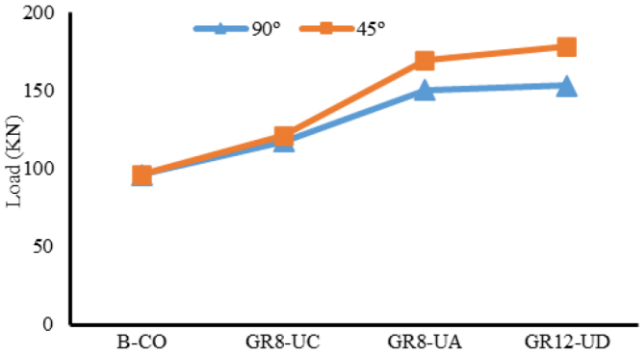

Fig. 11 the effect of spacing between GFRP rods stirrups

Fig. 7(i). the beam (GS8-UR-90) failed due to GFRP rupture at the bottom as show in Fig. 7(j).

3.3 Discussion

3.3.1 Effect of the spacing between stirrups

Fig. 11 showed the effect of spacing between GFRP rods stirrups., as the spacing between the NSM GFRP rods in the orthogonal direction decreases, the carrying load capacity increases, But at a low rate. As the spacing between the NSM GFRP rods in the orthogonal direction is decreased the interaction between the bond stresses around adjacent GFRP stirrups gets strengthened and hence the formation of failure pattern is accelerated. Thus, decreasing the spacing between the stirrups do not benefit the load capacity of the beams. In both cases, the reduced distance strengthens the interaction between the bond stresses around adjacent stirrups and hence accelerates the formation of failure patterns.

3.3.2 Effect of the alignment of the stirrups with NSM

Fig. 12 showed the effect of the alignment of GFRP rods stirrups. at the specimens strengthened with inclined GFRP rods, an increase in carrying load capacity was observed more than specimens strengthened with vertical GFRP rods. It is also observed that inclined rods were more effective than vertical rods. This is justified by the orientation of the shear failure cracks that had a tendency to be almost orthogonal to inclined laminates. Furthermore, for vertical rods, the total resisting bond length of the GFRP is lower

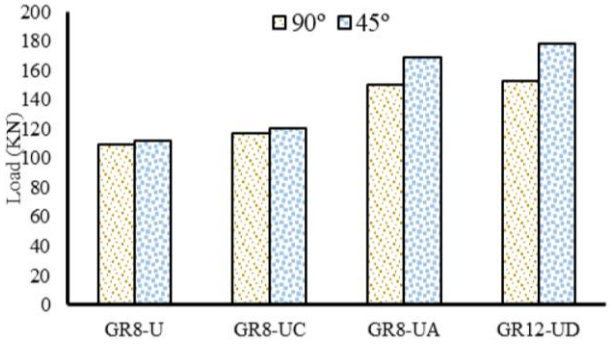

Fig. 12 the effect of the alignment of GFRP rods stirrups

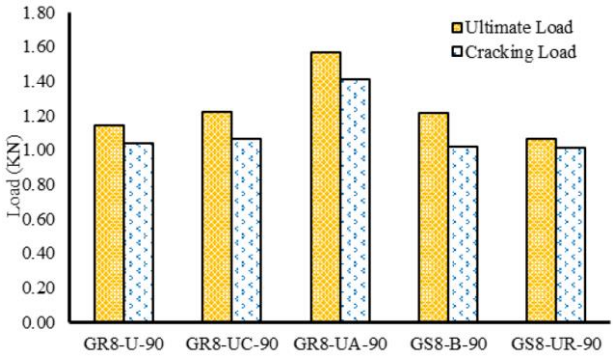

Fig. 13 the influence of add the end anchorage at the of GFRP rods stirrups

than that of inclined rods.

3.3.3 Effect of the end anchorage

Figs. 13 and 15 shown the influence of adding the end anchorage at the GFRP rods stirrups on the carrying load capacity and cracking load capacity and deflection. It is clear that the specimens strengthened with rods GFRP with end anchorage showed much better results than the other specimens. the carrying load capacity and cracking load was increased by 37%, 36% compared to specimen (GR8-U-90) with GFRP rods without end anchorage, the deflection corresponding to the ultimate and crack load in specimen (GR8-UA-90) with anchored GFRP was increased by 70%, 98% compared to specimen (GR8-U-90) without end anchorage. it was due to the increased in the debonding length between GFRP rods and the concrete

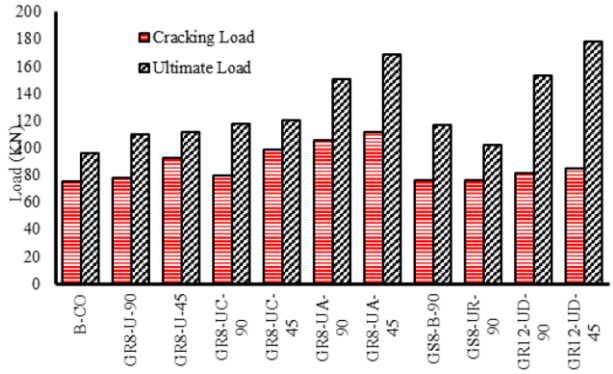

Fig. 14 the influence of the shear reinforcement technique on ultimate load and cracking load

surface. Clearly, the use of GFRP rods with end anchorage in (GR8-UA-90) and (GR8-UA-45) specimens led to an enhancement in both the ultimate strength and the corresponding deflection.

3.3.4 Effect of the strengthening technique

Fig. 14 shown the influence of the shear reinforcement technique on the ultimate load and crack load. the NSM technique was the most effective among the adopted GFRP shear strengthening configurations, and the EBR was the least effective configuration. the specimens strengthened with GFRP rods with the NSM technique showed significant improvement in the ultimate load and cracking load between (14% and 85%), (1% and 45%) larger than the (B-CO) beam, respectively. While the increase was low in the ultimate load in specimens strengthened with the EBR technique 7% and 22%, While the cracking load showed no improvement.

3.3.5 Effect of the strengthening technique on the deformability indices

Fig. 15 shown the influence of the shear strengthening technique on deformation capacity. Clearly, the use of GFRP rods with end anchorage led to an enhancement in the ultimate deflection and crack deflection. The highest deformation capacity was registered in the specimens strengthened with GFRP rods with end anchorage (GR8-UA-45), (GR8-UA-45). At both the deflection corresponding ultimate load and crack load. In comparison

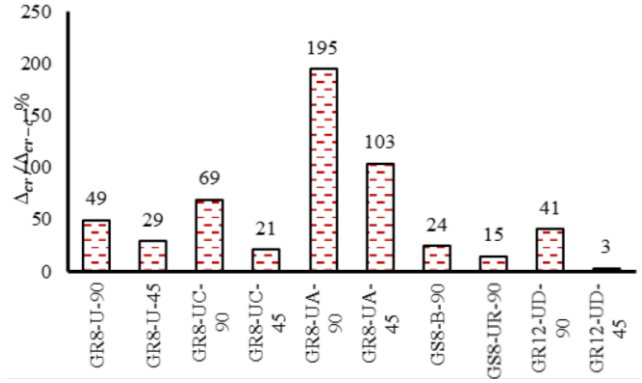

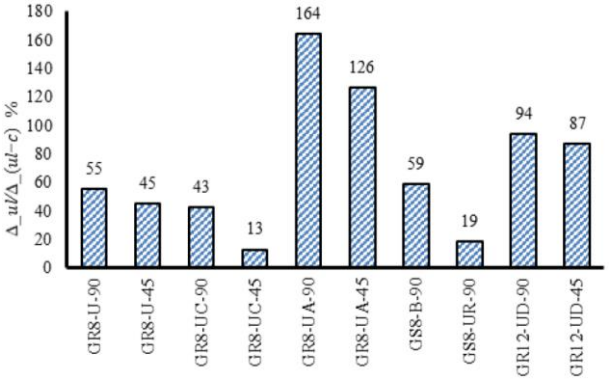

Fig. 15 the influence of the shear strengthening technique on deformation capacity

with (B-CO) specimen (unreinforced beam) is between 164%, 126% and 195%, 103% larger. Respectively.

4. Conclusions

From the study conducted on the shear strengthening of reinforced concrete beams (R.C) using near surface mounted (NSM) technique using GFRP in different types like rods, strips. in different alignments and spacing's and different end anchorage; From this study, the following conclusions can be made:

- GFRP rods, strips are found to be effective in the shear strengthening of reinforced concrete beams RC.
- The strengthened specimens showed improvement in all terms like deflection characteristics, first crack load, and ultimate load when compared to the control specimen.
- The use of near surface mounted (NSM) technique was more efficient than externally bonded reinforcement technique (EBR) in shear strengthening. When compared between the shear capacity of RC beams strengthened with NSM with those of RC beams externally bonded reinforcement with GFRP side sheets with the same amount of fiber Confirmed that the performance of the NSM better than EBR side strips.
- The ultimate shear of all the strengthened beams was more than that of the control beam.
- the samples strengthened with (NSM) technique by using GFRP rods U shape with anchorage, showed an improvement in the ultimate load compared to the samples strengthened with (NSM) technique by using GFRP rods U shape without a cap. But when compared with the control sample, the load was improved Significantly. The increase in the shear capacity was between 57% and 76% for these specimens.
- the specimens strengthened with (NSM) technique by using GFRP rods U-shape with strand, showed an improvement in the ultimate load compared to the control specimens, As a result of the reduction of the distance between the GFRP rods. The increase in the shear capacity was between 59% and 85% for these specimens.
- The test results have confirmed that the use of anchorage at the end of rods is effective for improving the shear capacity of reinforced concrete beams.

Acknowledgment

The authors wish to offer their sincere gratitude to the staff of reinforced concrete laboratory of the department of Civil Engineering, Benha University, Benha, for their support and collaboration during the course of this research.

References

Al-Salloum, Y.A., El-Gamal, S., Almusallam, T.H., Alsayed, S.H. and Aqel, M. (2013), "Effect of harsh environmental conditions on the tensile properties of GFRP bars", *Compos. Part B: Eng.*, **45**(1), 835-844. https://doi.org/10.1016/j.compositesb.2012.05.004.

Al Rjoub, Y.S., Ashteyat, A.M., Obaidat, Y.T. and Bani-Youniss, S. (2019), "Shear strengthening of RC beams using near-surface mounted carbon fibre-reinforced polymers", *Austr. J. Struct. Eng.*, 1-9. https://doi.org/10.1080/13287982.2019.1565617.

Baji, H., Eslami, A. and Ronagh, H.R. (2015), "Development of a nonlinear FE modelling approach for FRP-strengthened RC beam-column connections", *Struct.*, **3**, 272-281. https://doi.org/10.1016/j.istruc.2015.06.003.

Bianco, V., Monti, G. and Barros, J.A. (2014), "Design formula to evaluate the NSM FRP strips shear strength contribution to a RC beam", *Compos. Part B: Eng.*, **56**, 960-971. https://doi.org/10.1016/j.compositesb.2013.09.001.

Dalalbashi, A., Eslami, A. and Ronagh, H.R. (2012), "Plastic hinge relocation in RC joints as an alternative method of retrofitting using FRP", *Compos. Struct.*, **94**(8), 2433-2439. https://doi.org/10.1016/j.compstruct.2012.02.016.

Dalalbashi, A., Eslami, A. and Ronagh, H.R. (2013), "Numerical investigation on the hysteretic behavior of RC joints retrofitted with different CFRP configurations", *J. Compos. Constr.*, **17**(3), 371382. https://doi.org/10.1061/(ASCE)CC.1943-5614.0000361.

De Lorenzis, L. and Teng, J.G. (2007), "Near-surface mounted FRP reinforcement: An emerging technique for strengthening structures", *Compos. Part B: Eng.*, **38**(2), 119-143. https://doi.org/10.1016/j.compositesb.2006.08.003.

Deng, J., Liu, A., Huang, P. and Zheng, X. (2016), "Interfacial mechanical behaviors of RC beams strengthened with FRP", *Struct. Eng. Mech.*, **58**(3), 577-596. http://doi.org/10.12989/sem.2016.58.3.577.

Dias, S.J. and Barros, J.A. (2010), "Performance of reinforced concrete T beams strengthened in shear with NSM CFRP laminates", *Eng. Struct.*, **32**(2), 373-384. https://doi.org/10.1016/j.engstruct.2009.10.001.

Dias, S.J. and Barros, J.A. (2013), "Shear strengthening of RC beams with NSM CFRP laminates: Experimental research and analytical formulation", *Compos. Struct.*, **99**, 477-490. https://doi.org/10.1016/j.compstruct.2012.09.026.

Eslami, A. and Ronagh, H.R. (2014), "Experimental investigation of an appropriate anchorage system for flange-bonded carbon fiber–reinforced polymers in retrofitted RC beam–column joints", *J. Compos. Constr.*, **18**(4), 04013056. https://doi.org/10.1061/(ASCE)CC.1943-5614.0000456.

Hassan, T. and Rizkalla, S. (2002), "Flexural strengthening of prestressed bridge slabs with FRP systems", *PCI J.*, **47**(1), 76-93.

Hassan, T. and Rizkalla, S. (2003), "Investigation of bond in concrete structures strengthened with near surface mounted carbon fiber reinforced polymer strips", *J. Compos. Constr.*, **7**(3), 248-257. https://doi.org/10.1061/(ASCE)1090-0268(2003)7:3(248).

Jayaprakash, J., Samad, A.A.A., Abbasovich, A.A. and Ali, A.A.A. (2008), "Shear capacity of precracked and non-precracked reinforced concrete shear beams with externally bonded bi-directional CFRP strips", *Constr. Build. Mater.*, **22**(6), 1148-1165. https://doi.org/10.1016/j.conbuildmat.2007.02.008.

Kachlakev, D. and McCurry, D.D. (2000), "Behavior of full-scale reinforced concrete beams retrofitted for shear and flexural with FRP laminates", *Compos. Part B: Eng.*, **31**(6-7), 445-452. https://doi.org/10.1016/S1359-8368(00)00023-8.

Khalifa, A. and Nanni, A. (2002), "Rehabilitation of rectangular simply supported RC beams with shear deficiencies using CFRP composites", *Constr. Build. Mater.*, **16**(3), 135-146. https://doi.org/10.1016/S0950-0618(02)00002-8.

Kocak, A. (2015), "Earthquake performance of FRP retrofitting of short columns around band-type windows", *Struct. Eng. Mech.*, **53**(1), 1-16. http://doi.org/10.12989/sem.2015.53.1.001.

Mosallam, A.S. and Banerjee, S. (2007), "Shear enhancement of reinforced concrete beams strengthened with FRP composite

laminates", *Compos. Part B: Eng.*, **38**(5-6), 781-793. https://doi.org/10.1016/j.compositesb.2006.10.002.

Moshiri, N., Tajmir-Riahi, A., Mostofinejad, D., Czaderski, C. and Motavalli, M. (2019), "Experimental and analytical study on CFRP strips-to-concrete bonded joints using EBROG method", *Compos. Part B: Eng.*, **158**, 437-447. https://doi.org/10.1016/j.compositesb.2018.09.046.

Mostofinejad, D. and Mahmoudabadi, E. (2010), "Grooving as alternative method of surface preparation to postpone debonding of FRP laminates in concrete beams", *J. Compos. Constr.*, **14**(6), 804-811. https://doi.org/10.1061/(ASCE)CC.1943-5614.0000117.

Ramezanpour, M., Morshed, R. and Eslami, A. (2018), "Experimental investigation on optimal shear strengthening of RC beams using NSM GFRP bars", *Struct. Eng. Mech.*, **67**(1), 45-52. http://doi.org/10.12989/sem.2018.67.1.045.

Rizzo, A. and De Lorenzis, L. (2009), "Behavior and capacity of RC beams strengthened in shear with NSM FRP reinforcement", *Constr. Build. Mater.*, **23**(4), 1555-1567. https://doi.org/10.1016/j.conbuildmat.2007.08.014.

Sundarraja, M.C. and Rajamohan, S. (2009), "Strengthening of RC beams in shear using GFRP inclined strips– An experimental study", *Constr. Build. Mater.*, **23**(2), 856-864. https://doi.org/10.1016/j.conbuildmat.2008.04.008.

Täljsten, B. and Elfgren, L. (2000), "Strengthening concrete beams for shear using CFRP-materials: evaluation of different application methods", *Compos. Part B: Eng.*, **31**(2), 87-96. https://doi.org/10.1016/S1359-8368(99)00077-3.

Zhang, Z. and Hsu, C.T.T. (2005), "Shear strengthening of reinforced concrete beams using carbon-fiberreinforced polymer laminates", *J. Compos. Constr.*, **9**(2), 158-169. https://doi.org/10.1061/(ASCE)1090-0268(2005)9:2(158).

CC